Tip-induced local anodic oxidation on the native SiO_2 layer of Si(111) using an atomic force microscope

Y.-R. Ma,[1,*] C. Yu,[2] Y.-D. Yao,[3] Y. Liou,[3] and S.-F. Lee[3]
[1]*Department of Physics, National Dong Hwa University, Hualien 974, Taiwan, Republic of China*
[2]*Department of Physics, National Taiwan University, Taipei 106, Taiwan, Republic of China*
[3]*Institute of Physics, Academia Sinica, Taipei 11529, Taiwan, Republic of China*
(Received 16 January 2001; revised manuscript received 23 July 2001; published 26 October 2001)

Atomic force mocroscope (AFM) tip-induced local anodic oxidation on a native SiO_2 layer of Si(111) which is in contact mode is presented in an ambient way. This local anodic oxidation was subjected to varying sample voltages. When an AFM tip was positioned on a surface point with various voltage pulses of 10 V point oxide protrusions were tip induced. The protruded height grew exponentially due to the duration. Large-area oxide bumps also become tip induced when an AFM tip was swept across large surface areas. The bump height increased and was linearly dependent on the sample voltage. Two possible approaches to local anodic oxidation on the native SiO_2 layer are discussed.

DOI: 10.1103/PhysRevB.64.195324 PACS number(s): 81.65.Mq, 68.37.Ps

I. INTRODUCTION

Various techniques, including thermal oxidization,[1] can be employed to oxidize semiconductors. Since the direct and local anodic oxidation of hydrogen-passivated *n*-type Si(111) surfaces in an ambient way using a scanning tunneling microscope (STM) was first presented,[2] creating surface oxide patterns within a nanometer scale has attracted significant interest in nanoelectronic devices—field effect transistors,[3–10] single-electron transistors,[11] as well as in other applications.[12–17] The atomic force microscope (AFM)/STM local tip-induced anodic oxidation has been applied to not only Si, but other materials, such as Ti,[5,11,13,18] Al,[14] Cr,[19] MoS_2,[12] TiN,[20] and Si_3N_4.[17,21] Many factors, such as tunneling current, scan speed, pulse duration and contact force, may affect local tip-induced anodization. However, it has been widely accepted[22–25] that a strong local electric field between tip and sample surface performs a significant function in initiating a local anodic oxidation in an ambient way.

In this work the AFM tip-induced local anodic oxidation on a native SiO_2 layer of Si(111) is presented in an ambient way. When an AFM tip rests on a surface point with a pulse of 10 V for the duration of an experiment, an oxide protrusion becomes tip induced. Applying various 10 V pulses to a surface point, the protruded oxide height grows as an exponential function of duration. When an AFM tip is scanned across a large surface area, a large-area oxide bump also becomes tip induced at varying voltages, which range from 4 V to 10 V. Furthermore, this bump height increases with a linear dependence on the sample voltages. Growth rate and kinetics of the local anodization on the native SiO_2 layer of Si(111) will be discussed regarding point and large-area oxidations.

II. EXPERIMENTS

Using an ambient AFM (Solver-P47 model, NT-MDT, Moscow, Russia) this experiment was performed at room temperature with humidity that ranged from $\sim 60\%$ to $\sim 68\%$. A commercial Si(111) sample of 7×7 mm^2 was cut from an *n*-type wafer (Sb dopant, resistivity $\sim 0.1\Omega$ cm), and the surface of Si(111) was capped with a thin native SiO_2 layer at room temperature with humidity at approximately $\sim 35\%$. The SiO_2 layer of Si(111) was cleaned and rinsed in acetone and alcohol for 5 min each in an ultrasonic bath, and then blown dry with nitrogen gas. AFM images were obtained in the contact mode via NT-MDT-made *p*-type silicon cantilevers (B dopant, resistivity $\sim 0.01\Omega$ cm) within a force constant 0.6 N/m. For point anodic oxidation, various 10 V pulses, which ranged from 1 to 100 sec, acted on various surface points through AFM tips. However, for large-area oxidation, AFM tips were scanned backward and forward across a large area with various sample voltages that ranged from 2 V to 10 V. The scan speeds were 5000 nm/s, 10 000 nm/s, 15 000 nm/s, and 20 000 nm/s, and the threshold voltage for the local anodic oxidation on the native SiO_2 layer of Si(111) was ~ 4 V, respectively.

III. RESULTS AND DISCUSSION

When an AFM tip contacts and rests on a surface point of the native SiO_2 layer, an oxide protrusion becomes tip induced due to a static voltage pulse of 10 V for the duration. Figure 1(a) shows an AFM image (8500×1000 nm^2) in which a series of point oxide protrusions, from left to right, are produced via 10 V pulses of 1, 5, 10, 30, 60, and 100 sec, respectively. Obviously, the average full width at half maximum of the point oxide protrusions is ~ 100 nm, and the protruded point oxide height increases concurrently with pulse time [Fig. 1(b)]. This indicates that point oxide growth follows the direction (perpendicular to the surface) of the electric field with time. Notably, this experimental result is similar to those presented previously[24,25] regarding anodic oxidation at varying static voltages and pulses for the duration.

To understand the effect of the quantitative voltage pulses, the point oxide heights were measured with an AFM profile function and averaged five times. Figure 2 shows a graph that compares the point oxide height and the voltage pulse duration. All data from the point oxide heights were curve

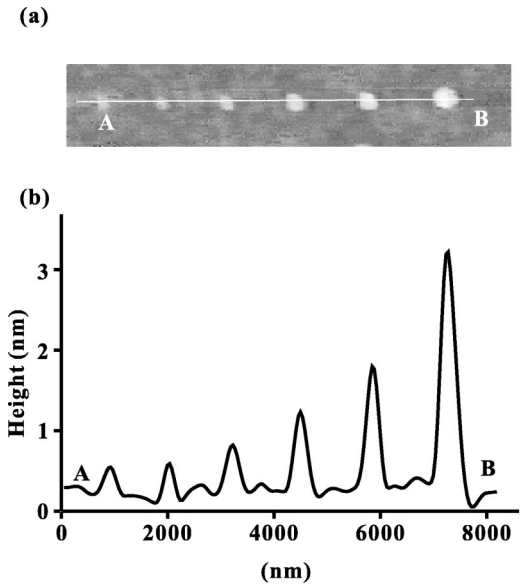

FIG. 1. (a) An AFM image ($8{,}500\times1{,}000$ nm^2) depicting a series of point oxide protrusions, from left to right, which were obtained at the 10 V pulses of 1, 5, 10, 30, 60, and 100 sec, respectively. (b) An outline of the *AB* line in (a) for the point oxide protrusion height.

fitted with an exponential growth, that is,

$$h=A-Be^{-t/\tau}, \tag{1}$$

where h and t represent the height and duration, A ($=3.2$) and B ($=2.9$) are initial constants, and τ ($=30$ sec) is the curve-fitted constant, respectively. Therefore, the growth rate becomes

$$dh/dt=(B/\tau)e^{-t/\tau}\cong 0.91e^{-t/30}. \tag{2}$$

Several reports[22–27] have proposed the local anodic oxidation mechanism via STM/AFM, i.e., the humidity and electric field between the tip and surface primarily affects the kinetic local anodic oxidation. A model of AFM/STM silicon oxidation has also been proposed.[28] This paper shows two possible approaches to local anodic oxidation on the native SiO_2 layer of Si (111), as shown in Fig. 3. Fig. 3(a) schematically illustrates an AFM tip resting on a surface point with a positive sample voltage. When a static 10 V pulse is initially applied, electrons accumulate on the apex of the AFM tip and equivalent positive charges are spontaneously induced at the Si/SiO_2 interface underneath the contact point; O^{2-} and OH^- are electrochemically generated at the air/SiO_2 interface. Pb paramagnetic centers exist at the Si/SiO_2 interface,[29,30] each center has Si atoms bonded to three other Si atoms with an unpaired electron. The structure of Pb is $\bullet Si\equiv Si_3$, where the dot and three parallel lines represent the unpaired electron and three discrete bonds. Concentrations of Pb paramagnetic centers have been reported[31] to be influenced by the oxidation temperature and cooling rate: the con-

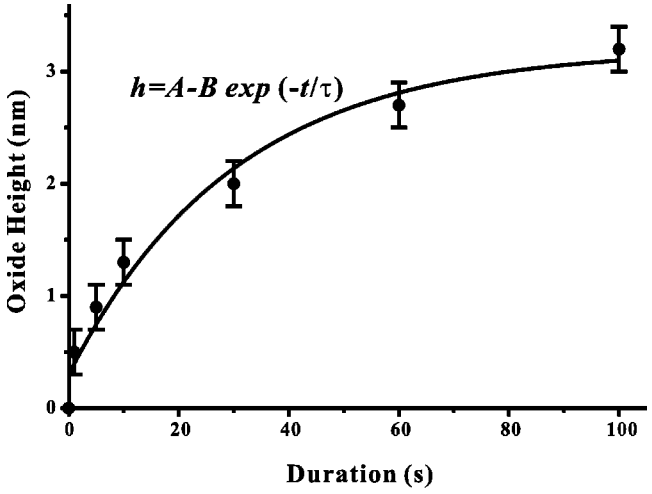

FIG. 2. A linear graph of point oxide height and voltage pulse duration.

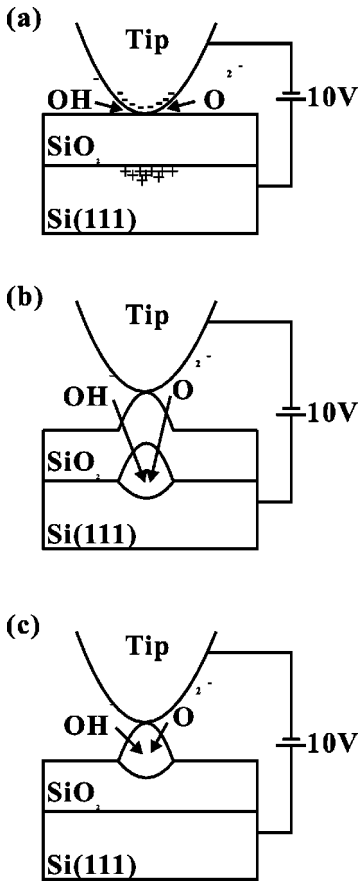

FIG. 3. Schematic diagrams of two possible approaches for the local anodic oxidation on the native SiO_2 layer of Si(111). (a) When an AFM rests on a surface point at the sample voltage of 10 V, electrons accumulate on the apex of the AFM tip and equivalent positive charges are induced spontaneously at the interface beneath the contact point. Water vapor (or adsorbed water) and oxygen gases are dissociated to produce OH^- and O^{2-} ions near the apex of the AFM tip. (b) A possible approach is that the OH^- and O^{2-} ions diffuse through the native SiO_2 layer and enter the interface via a strong electric field between tip and sample, and an oxide then grows at the interface. (c) The other approach is that the OH^- and O^{2-} ions cannot completely diffuse through the native SiO_2 layer, but rather remain inside the oxide layer to form an oxide protrusion.

centration of Pb paramagnetic centers is reduced when Pb paramagnetic centers are terminated by hydrogen-related impurities, such as H and OH, during oxidation of Si wafers to form passivated structures, H-Si≡Si_3 (labeled PbH) or H-O-Si≡Si_3 (labeled PbOH). Based on an anodizing model proposed by Gordon *et al.*,[23] water vapor (or adsorbed water) and oxygen gas were dissociated to produce OH^- and O^{2-} ions, which diffused through the native SiO_2 layer: ion diffusion is enhanced by AFM tips, which support a powerful electric field, and the anodic oxidation occurs at the Si/SiO_2 interface [Fig. 3(b)]. As the OH^- and O^{2-} ions diffuse through the native SiO_2 layer and enter the Si/SiO_2 interface, they begin to react with the passivated PbH or PbOH centers following the oxidation processes described in the model of Gordon *et al.*[23] Here, the tip-induced local positive charges neutralize the OH^- and O^{2-} ions. However, when a point oxide occurs at the Si/SiO_2 interface, the expansion of volume causes stress at a limited local space in the Si/SiO_2 interface. The point oxide pushes the native SiO_2 layer upward to form a protrusion, and releases the extension stress. Therefore, the thickness of the native SiO_2 layer restricts the growth of the point oxide. A greater thickness of the oxide protrusion corresponds to a weaker electrical field, which also limits point oxide growth.

In addition, Fig. 3(c) depicts another approach to the point oxide protrusion. The OH^- and O^{2-} ions cannot diffuse completely through the native SiO_2 layer, but rather remain inside the oxide layer. This phenomenon is similar to that of ion implantation, in that the diffusing OH^- and O^{2-} ions disrupt the silicon compound and react to produce amorphous silica. In contrast to the native SiO_2 layer that has the crystalline nature of quartz, the amorphous silica contains much disorder. The structure of SiO_2 is based on a network of SiO_4 tetrahedra with shared oxygen atoms, whereas the structure of amorphous silica may contain arrangements of the interconnected SiO_4 tetrahedra, such as silicate structures. Silicates have O/Si ratios exceeding 2:1, so that the expansion of volume happens at a local surface of the native SiO_2 layer to form an oxide protrusion. In addition, E' paramagnetic centers have been found in silicon oxide;[30–32] each center is an Si atom bonded to three O atoms with an unpaired electron. The structure of E' paramagnetic centers is ●Si≡O_3, where the dot and three parallel lines represent the unpaired electron and three discrete bonds. When the OH^- and O^{2-} ions diffuse into the native SiO_2 layer, these ions react with E' paramagnetic centers to give polyatomic silicon-oxygen anions, possibly enhancing the expansion of volume. While the rate of ion diffusion is unclear, an increase in oxide thickness or decrease in electrical-field strength may reduce this rate.

To more thoroughly understand the local tip-induced anodic oxidation, large-area oxidation by means of a moving tip is presented. When an AFM tip scans a surface area, large-area oxide bumps are produced at sample voltages that exceed the threshold voltage (=4 V). Notably, the voltage pulse duration that is applied to every surface point (256 ×256 points) is 2 ms. In Fig. 4(a) an AFM image (13,100 ×9300 nm^2) reveals that there is an array of 12 rectangular

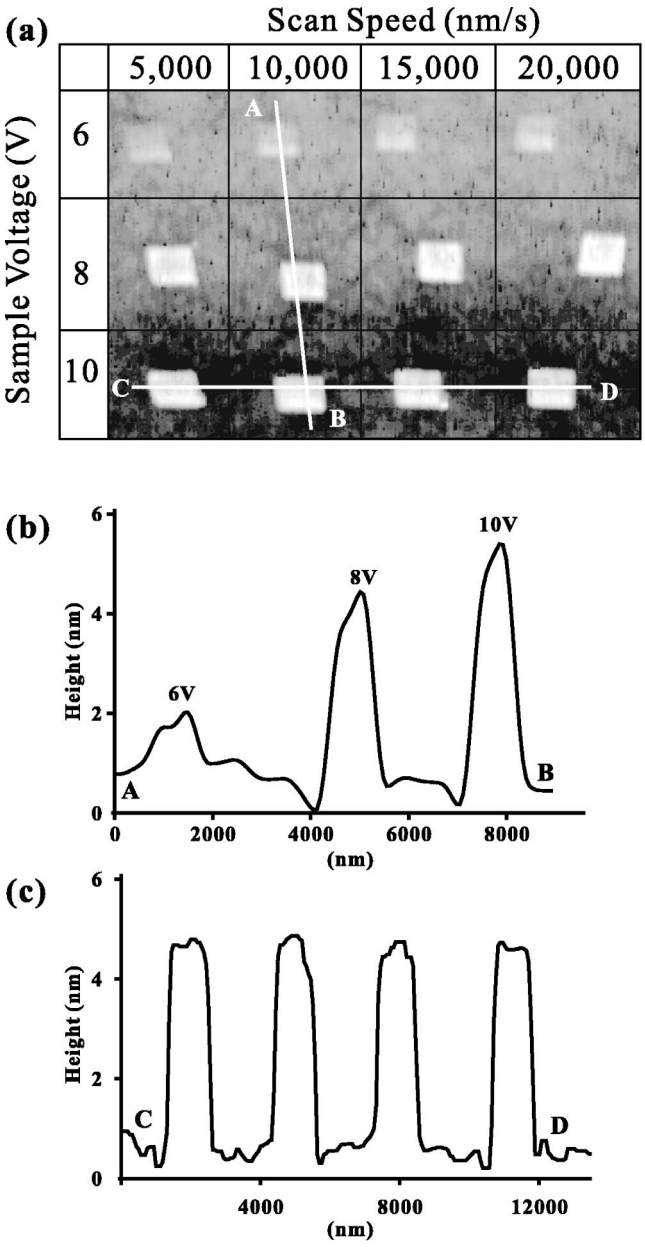

FIG. 4. (a) An AFM image (13100×9300 nm^2) displaying an array of 12 rectangular large-area oxide bumps on a native SiO_2 layer of Si(111). Two graphs in (d) and (c) present two outlines of the *AB* and *CD* lines in (a).

large-area oxide bumps on the native SiO_2 layer of Si(111). The average size of the large-area oxide bumps is ~1100 ×950 nm^2. Figure 4(a) displays three rows of the large-area oxide bumps, from top to bottom, which were obtained at the sample voltages, 6 V, 8 V, and 10 V. However, various scan speeds, 5000 nm/s, 10 000 nm/s, 15 000 nm/s, and 20 000 nm/s, respectively, were employed. Two lines, from *A* and *B* and from *C* and *D*, pass through three and four oxide bumps. Figures 4(b) and 4(c) illustrate the two outlines of these *AB* and *CD* lines. These figures also confirm that the heights of the three large-area oxide bumps are proportional to the positive sample voltages but independent of the scan speeds. This experimental result accords with those presented

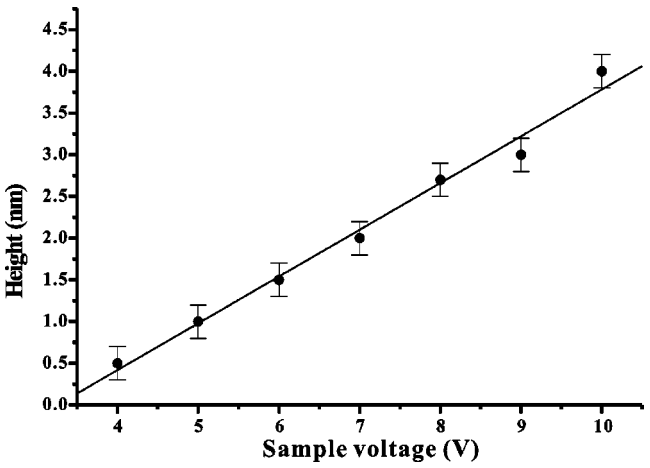

FIG. 5. A linear graph of height and sample voltage.

previously.[26,27] Figure 5 demonstrates a graph, which compares height to sample voltage. A linear line with error bars of 0.2 nm fit all data from the large-area oxide heights. It indicates that the height of the large-area oxide bump is linearly dependent on the sample voltage.

In addition, comparing Fig. 2 to Fig. 5, the height of the large-area oxide bump obtained at 10 V is ~ 4 nm greater than that of the point oxide protrusion obtained at a static 10 V pulse of 100 sec, hence indicating that the growth limitation of the former differs from that of the latter. When an AFM tip contacts an initial point on the surface, a point oxide protrusion occurs at an applied pulse of a static voltage (threshold voltage). As the tip begins to scan the surface forward from the initial point, a series of point oxide protrusions appears at sequential static voltage pulses. Here, the latter point oxide protrusions are higher than the former ones. This is due to the latter point oxide protrusions, which grow constantly at a range of the neighboring voltage pulses, until the voltage pulse power is terminated. When the tip sweeps back and forth, the growth process repeatedly forms a large-area oxide bump. According to two growth approaches presented in Fig 3(b) and 3(c), this oxide bump may grow at the interface, or on the surface. Therefore, via magnitude and pulse control of the applied voltage, oxide protrusion or bumps are produced within the gate oxide, which can be further applied for nanodevice fabrication.

IV. CONCLUSIONS

Growth of point and large-area anodic oxidations on the native SiO_2 layer of Si(111) were presented. The protruded height grew exponentially as a function of duration, and the bump height increased due to a linear dependence on the sample voltage. Two approaches were proposed for the oxide growth mechanism, that is, OH^- and O^{2-} ions undergoing a strong electrical field diffuse through the native SiO_2 layer to form oxides at the Si/SiO_2 interface or in the native SiO_2 layer.

ACKNOWLEDGMENTS

The authors would like to acknowledge fruitful discussions with Dr. C.-L. Chien (Department of Chemistry, National Dong Hwa University, Hualien, 974, Taiwan, R.O.C.). This work was financially supported by the National Science Council of the Republic of China (NSC-89-2112-M-259-016).

*Corresponding author. Email address: ronma@mail.ndhu.edu.tw

[1] S.M. Sze, *Semiconductor Devices, Physics and Technology* (Wiley, New York, 1985), p 342.
[2] J.A. Dagata, J. Schneir, H.H. Harary, C.J. Evans, M.T. Postek, and J. Bennet, Appl. Phys. Lett. **56**, 2001 (1990).
[3] S.C. Minne, H.T. Soh, Ph. Flueckiger, and C.F. Quate, Appl. Phys. Lett. **66**, 703 (1995).
[4] P.M. Campbell E.S. Snow, and P.J. McMarr, Appl. Phys. Lett. **66**, 1388 (1995).
[5] M.S. Hagedom, D.D. Litfin, G.M. Price, A.E. Gordon, and T.K. Higman, J. Vac. Sci. Technol. B **14**, 4153 (1996).
[6] P.M. Campbell and E.S. Snow, Semicond. Sci. Technol. **11**, 1558 (1996).
[7] P.M. Campbell, E.S. Snow, and P.J. McMarr, Physica B **227**, 315 (1996).
[8] P.M. Campbell E.S. Snow, and P.J. McMarr, Surf. Sci. **361/362**, 870 (1996).
[9] P.M. Campbell and E.S. Snow, Mater. Sci. Eng., B **B51**, 173 (1998).
[10] E.S. Snow and P.M. Campbell, *Materials—Fabrication and Patterning at the Nanoscale*, edited by C.R.K. Marrian, K. Kash, F. Cerrina, and M. Lagally, MRS Symposia proceedings (Mater. Res. Soc. Symp. Proc. 380, Materials Research Society, Pittsburgh, 1995), p. 131.
[11] K. Matsumoto, M. Ishii, K. Segawa, Y. Oka, B.J. Vartanian, and J.S. Harris, Appl. Phys. Lett. **68**, 34 (1996).
[12] Y. Kim and C.M. Lieber, Science **257**, 375 (1992).
[13] E.S. Snow and P.M. Campbell, Science **250**, 1639 (1995).
[14] E.S. Snow, D. Park, and P.M. Campbell, Appl. Phys. Lett. **69**, 269 (1996).
[15] E.S. Snow, W.H. Juan Park, S.W. Pang, and M. Campbell, Appl. Phys. Lett. **66**, 1729 (1995).
[16] R. Held, T. Heinzel, P. Studerus, K. Ensslin, and M. Holland, Appl. Phys. Lett. **71**, 2689 (1997).
[17] T. Yasuda, S. Yamasaki, and S. Gwo, Appl. Phys. Lett. **77**, 3917 (2000).
[18] H. Sugimura, T. Uchida, N. Kitamura, and H. Masuhara, Appl. Phys. Lett. **63**, 1288 (1993).
[19] D. Wang, L. Tsau, and K.L. Wang, Appl. Phys. Lett. **67**, 1295 (1995).
[20] S. Gwo, C.-L. Yeh, P.-F. Chen, Y.-C. Chou, and T.T. Chen, Appl. Phys. Lett. **74**, 1090 (1999).
[21] F.S.-S. Chien, J.-W. Chang, S.-W. Lin, Y.-C. Chou, T.T. Chen, S. Gwo, T.-S. Chao, and W.-F. Hsieh, Appl. Phys. Lett. **76**, 360 (2000).
[22] H. Sugimura, T. Uchida, N. Kitamura, and H. Masuhara, J. Phys. Chem. **98**, 4352 (1994).
[23] A.E. Gordon, R.T. Fayfield, D.D. Litfin, and T.K. Higman, J. Vac.

Sci. Technol. B **13**, 2805 (1995).
[24] Ph. Avouris, T. Hertel, and R. Martel, Appl. Phys. Lett. **71**, 285 (1997).
[25] R. Garcia and M. Calleja, Appl. Phys. Lett. **72**, 2295 (1998).
[26] D. Stievenard, P.A. Fontaine, and E. Dubois, Appl. Phys. Lett. **70**, 3272 (1997).
[27] T. Teuschler, K. Mahr, S. Miyazaki, M. Hundhausen, and L. Ley, Appl. Phys. Lett. **67**, 3144 (1995).
[28] J.A. Dagata, T. Inoue, J. Itoh, and H. Yokoyama, Appl. Phys. Lett. **73**, 271 (1998).
[29] Y. Nishi, Jpn. J. Appl. Phys. **10**, 52 (1971).
[30] P. Caplan, E. Poindexter, B. Deal, and R. Razouk, J. Appl. Phys. **50**, 5847 (1979).
[31] K. Awazu, K. Watanabe, and H. Kawazoe, J. Appl. Phys. **73**, 8519 (1993).
[32] R. Weeks, and C. Nelson, J. Am. Ceram. Soc. **43**, 396 (1943).